

# Does MRI diffusion help in the detection and characterization of benign and malignant hepatic focal lesions in the nonpediatric age group?

Ahmed A. Mahmoud<sup>a</sup>, Marwa S. Elnafarawy<sup>b</sup>, Medhat M. Madbouly<sup>a</sup>,  
Mohammed H. Kamel<sup>a</sup>

<sup>a</sup>Department of Radiodiagnosis, Theodor Bilharz Institute, Giza, <sup>b</sup>Department of Radiodiagnosis, Cairo University, Cairo, Egypt

Correspondence to Ahmed A. Mahmoud, MD, Building 2103, Department of Radiology, Theodor Bilharz Research Institute, Palm Parks Compound, 6 October City, Egypt.  
Tel: +20 106 665 6633;  
e-mail: ahmedabdelsamie71@gmail.com

**Received:** 29 March 2020

**Revised:** 16 June 2020

**Accepted:** 16 July 2020

**Published:** 16 September 2020

**Kasr Al Ainy Medical Journal** 2020, 26:14–20

## Introduction

Liver MRI has been used in cases where ultrasound or computed tomography findings are equivocal. Diffusion-weighted imaging (DWI) established an important role in clinical use in the liver. DWI can potentially add useful information to conventional imaging.

## Objective

The aim was to assess the role of DWI in the detection and characterization of hepatic focal lesions and its value to differentiate benign from malignant masses.

## Patients and methods

The study included 40 patients, 19 women and 21 men, their ages ranged from 20 to 63 years. All patients underwent detailed MRI study of the abdomen.

Diffusion study was performed with tridirectional diffusion gradients using  $b$  values 0, 500, and 1000 s/mm<sup>2</sup> to increase the sensitivity. Apparent diffusion coefficient (ADC) maps and values were calculated for all lesions.

## Results

In all, 20 patients were diagnosed to have benign lesions and 20 patients were diagnosed to have malignant lesions.

Hemangiomas and cysts showed facilitated diffusion while adenomas show restricted diffusion pattern mimicking malignant focal lesions.

On the other hand, all malignant lesions showed restricted diffusion evidenced by increased signal on increasing the  $b$  values and low signal on ADC maps. Mostly benign lesions show higher ADC values than malignant lesions.

## Conclusion

Diffusion-weighted MRI sequence with quantitative ADC measurements should be used as an additional sequence to supplement conventional MRI protocol studies for proper characterization of focal hepatic lesions putting into consideration an overlap range.

## Keywords:

abdomen, liver, MR diffusion, tissue characterization

Kasr Al Ainy Med J 26:14–20

© 2020 Kasr Al Ainy Medical Journal

1687-4625

## Introduction

Hepatic focal lesions constitute daily diagnostic challenge. Liver (MRI) has been used in problematic cases as established by the most recent recommendations in the literature [1].

Diffusion-weighted imaging (DWI) established its role in clinical use in the liver. DWI can potentially add qualitative and quantitative information to conventional imaging. It is an unenhanced fast technique and easily incorporated to existing protocols [2].

The aim of this study was to assess the role of DWI in the detection and characterization of hepatic focal lesions and differentiate benign from malignant masses.

## Patients and methods

The study included 40 patients, 19 women and 21 men; their ages ranged from 20 to 63 years. The patients were referred from the Tropical and Surgery Departments to Radiology Department in Kasr Al-Ainy. All the patients had a focal hepatic lesion documented by ultrasound (US) and/or computed tomography (CT) scan. All cases had been subjected to the following:

- (1) Full clinical assessment.

This is an open access journal, and articles are distributed under the terms of the Creative Commons Attribution-NonCommercial-ShareAlike 4.0 License, which allows others to remix, tweak, and build upon the work non-commercially, as long as appropriate credit is given and the new creations are licensed under the identical terms.

- (2) Checking the patient's laboratory investigations including renal function tests (urea and creatinine).
- (3) Checking the previous radiological investigations done for the patient.

The study was approved by the Ethics Committee of our institution and written consent was taken from all patients.

Exclusion criteria:

- (1) Contraindications to contrast media, for example, patients with renal failure, patients allergic to contrast media.
- (2) Contraindications to MRI, for example, claustrophobia in patients contraindicated for anesthesia, non-MR-compatible cardiac prosthesis, pacemakers, metallic plates.
- (3) Previous interventional procedures such as TACE, RF, or microwave ablation.

Then they underwent detailed MRI study of the abdomen.

#### MRI protocol

The MR examination was performed on a high-field system 1.5 Tesla magnet unit (1.5 Tesla) using a Torso 16-channel coil. The study included conventional MRI, diffusion, and post-Gd-DTPA dynamic MR imaging. The conventional study included T1, T2, heavy T2, in-phase and out-of-phase sequences. The dynamic study was performed after bolus injection of 0.1 mmol/kg body weight of Gd-DTPA at a rate of 2 ml/s, flushed with 20 ml of sterile 0.9% saline solution via an antecubital vein. Dynamic imaging using ultrafast T1 fat-suppressed sequence including precontrast injection, arterial phase (16–20 s), arteriportal phase (20–40 s), and portovenous phase (45–60 s). This was followed by the delayed phase (2–3 min) after contrast injection.

Diffusion study was performed using respiratory-triggered fat-suppressed single-shot Echo planar DW imaging was performed in the transverse plane with tri-directional diffusion gradients using *b* values 0, 500, and 1000 s/mm<sup>2</sup> to increase sensitivity to cellular packing. The other parameters were as follows: repetition time (TR)=1880 ms, echo time (TE)=70 ms, number of excitations (NEX)=3, matrix 256×256 with a field of view as small as possible with 52% rectangular field of view, slice thickness 7–8 mm, slice gap 1–2 mm, and scan time 3–4 min.

#### Image analysis

Imaging evaluation assessed the morphological features of each lesion including size, shape, margin, signal characteristics, and dynamic pattern of enhancement as well as number and site of the detected focal lesions. Then provisional diagnosis was reported. Second, we reviewed the diffusion images for final radiological characterization and detection of focal lesions.

Apparent diffusion coefficient (ADC) maps and values were calculated for all lesions. One region of interest (1 cm) was applied to small lesions. For large lesions few regions of interest were applied and ADC measurements were averaged. The ADC data was accomplished by an automated application available on the scanner. The final diagnoses were reached according to the standard of reference (SOR). The SOR included two different imaging modalities, laboratory, clinical, and histopathological data.

#### Results

Our study included 40 patients, 19 (47.5%) women and 21 (52.5%) men. The patients' age ranged from 20 to 63 years with most of the patients lying in the group of 50 years and over. A total of 20 patients were diagnosed to have benign lesions and 20 patients were diagnosed to have malignant lesions.

The study included lesions of different sizes that ranged from small subcentimetric lesions to large infiltrative lesions (Table 1).

#### The final diagnoses were reached according to the standard of reference

For lesion characterization all imaging results were refined against a predefined SOR. A range of procedures were identified as valid 'gold standards' for the characterization of lesions. The ethically accepted and valid SOR for the hepatocellular carcinoma (HCC) lesions were the characteristic enhancement pattern on CT and/or MRI and elevated  $\alpha$ -fetoprotein. Hepatic cysts were diagnosed with typical US and/or CT and MRI findings. Hemangiomas were diagnosed easily with their

**Table 1** Range of size of different types of focal hepatic lesions

Type of lesions	Range of size (cm)
Cyst	1–4
Hemangioma	2–5
Adenoma	3–6
Hepatocellular carcinoma	3–7
Cholangiocarcinoma	4–7
Metastasis	0.5–5

characteristic US and/or MRI findings and unchanged mass dimensions on subsequent radiological procedures. Adenomas were diagnosed by their CT and MRI findings as well as their histopathological assessment. The metastatic lesions that were encountered in the study were patients with known primary malignancy (breast cancer, colorectal cancer, and pancreatic cancer) and with diagnosed metastasis, as they were discovered during routine screening. Cholangiocarcinomas were diagnosed by CT, MRI, and histopathological findings. The biopsy for histopathologically proven cases were performed either via CT or US-guided biopsy.

The benign lesions were cysts, hemangiomas, and adenomas. The malignant lesions were HCC, cholangiocarcinoma, and metastasis (Table 2).

All cysts and hemangiomas showed facilitated diffusion, either showing reduction of signal intensity on increasing the *b* values (85% of lesions) and those which did not show reduction of signal demonstrated high signal on the ADC map, which also reflects facilitated diffusion (15%). The adenomas yet show restricted diffusion pattern mimicking malignant lesions.

On the other hand, all malignant lesions showed restricted diffusion evidenced by increased signal on increasing the *b* values and low signal on ADC maps.

Mostly benign lesions show higher ADC values than malignant lesions.

The average ADC value for cysts was  $2.71 \times 10^{-3}$  (nine lesions, 22.5%).

The average ADC value for hemangiomas was  $2.1 \times 10^{-3}$  (eight lesions, 20%).

The average ADC value for adenomas was  $1.32 \times 10^{-3}$  (three lesions, 7.5%).

**Table 2 Different types of focal hepatic lesions, their number, percentage, and ADC range**

Type of lesion	Number of patients	%	ADC range
Cyst	9	22.5	$2.71 \times 10^{-3}$
Hemangioma	8	20	$2.1 \times 10^{-3}$
Adenoma	3	7.5	$1.32 \times 10^{-3}$
Hepatocellular carcinoma	7	17.5	$1.25 \times 10^{-3}$
Cholangiocarcinoma	3	7.5	$1.54 \times 10^{-3}$
Metastasis	10	25	$0.97 \times 10^{-3}$

ADC, apparent diffusion coefficient.

The average ADC value for HCCs was  $1.25 \times 10^{-3}$  (seven lesions, 17.5%).

The average ADC value range for cholangiocarcinomas was  $1.54 \times 10^{-3}$  (three lesions, 7.5%).

The average ADC value range for metastasis was  $0.97 \times 10^{-3}$  (10 lesions, 25%).

However, relatively high ADC values were encountered in few malignant lesions (three cholangiocarcinomas and two HCCs) measuring from  $1.4 \times 10^{-3}$  to  $1.79 \times 10^{-3}$ .

The above-mentioned data denotes an overlap range of ADC values between adenomas and few malignant lesions with no definite cutoff for the ADC value.

## Discussion

DWI shows promising results for hepatic focal lesion characterization. It is performed relatively quickly (two breath-hold acquisitions). It does not require contrast agent administration, so it can be performed in patients with severe renal insufficiency. The most used parameter for quantification in DWI for abdominal assessment is the ADC value requiring at least two *b* values (a low and a high *b* value) [3].

Although dynamic contrast-enhanced examinations have become a routine component of abdominal imaging, the high cost/benefit ratio and risk of contrast media side effects remain an issue [4].

In this study, diffusion images were obtained before intravenous contrast administration which was also mentioned by Wei C which stated that DW MR imaging of the liver is usually performed before contrast material administration, although performing DW MR imaging after the administration of contrast did not appear to significantly affect ADC calculations [4].

In this study, three different *b* values were conducted which was in line with the study performed by Caraiani *et al.* [1], although Kaya and Koc [2] stated that the use of only two *b* values (one of which is low and the other is high) can lead to ADC calculation ( $\geq$ two values).

Wei C stated that the disadvantage of using multiple *b* values is an associated increase in scanning time. The three *b* values used were *b*<sub>0</sub>, *b*<sub>500</sub>, and *b*<sub>1000</sub> [4].

DWI obtained using low  $b$  values increases lesion detection by suppressing normal liver signal intensity. A significant ADC difference was reported between benign and malignant liver lesions [5].

Malignant focal lesions, such as HCC nodules or metastases, present a pattern known as 'restricted diffusion,' that is, hyperintensity on the DWI image and hypointensity on the ADC map [5].

In our study, we used high  $b$  values as 500 and 1000  $\text{mm}^2/\text{s}^2$  in tissue characterization. Jahic *et al.* [6] mentioned that the use of high  $b$  value (500 and 1000  $\text{s}/\text{mm}^2$ ) minimizes the effect of capillary perfusion and water diffusion in extracellular extra vascular space, so a high  $b$  value will result in the reduction of signal from moving protons. This will result in increased contrast between the lesion and the liver and, furthermore, in differences in relative contrast ratio between malignant and benign lesions.

#### Regarding the size of lesions

Using low  $b$  value aids in the detection of focal lesions especially the small ones ( $\leq 1$  cm). This was shown in one of our cases which was a patient with multiple hepatic metastasis from colorectal carcinoma. The metastasis were detected by the low  $b$ -value diffusion

images and this was consistent with Colagrande *et al.* [7]. Calistri *et al.* [8] also mentioned in their study that the DWI detected more lesions than dynamic images concerning the small focal lesions ( $< 1$  cm).

As concerning the larger focal lesions ( $> 1$  cm), the diffusion images detected a large focal lesion which proved later to be HCC and was not evident in the T1 and T2WI (Fig. 1). This agreed with a study done by Colagrande *et al.* [7] and stated that DW imaging was associated with a higher detection rate of both malignant and benign focal lesions [7].

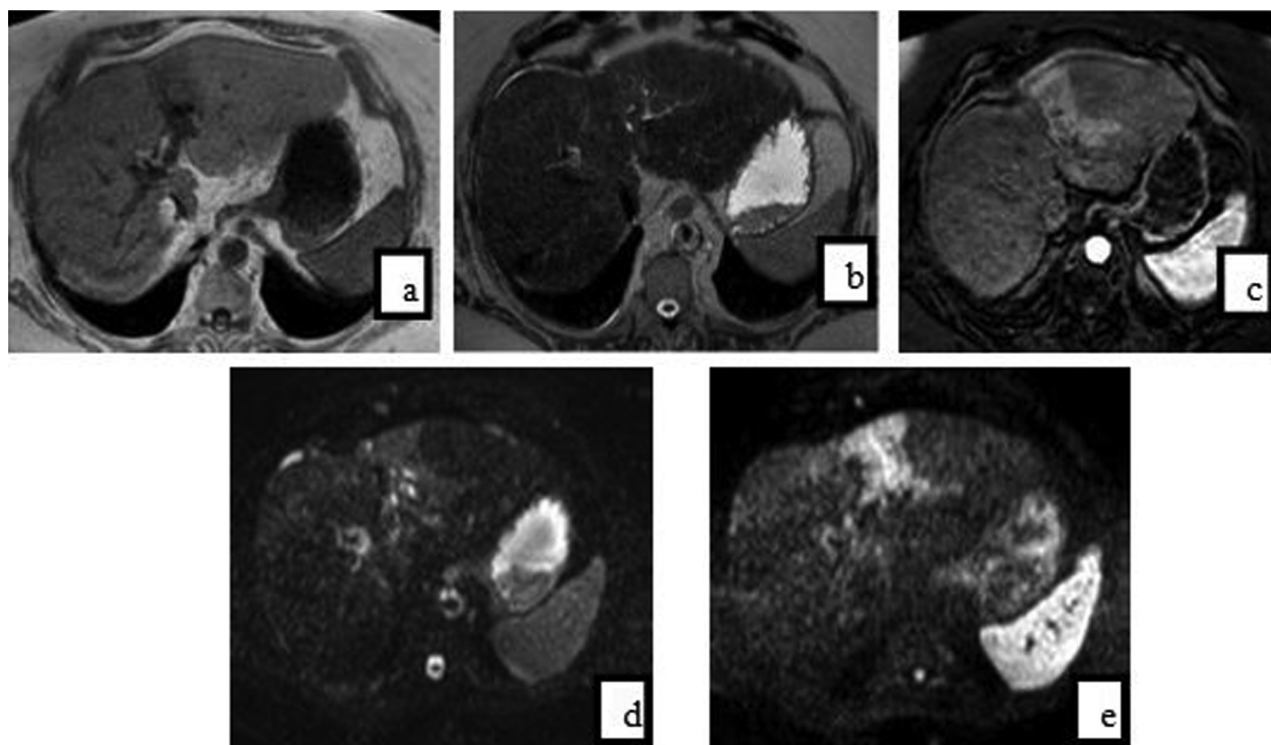
#### Regarding the number of lesions

There was no statistical significance concerning the detection of lesions according to their number as DWIs detected multiple and single lesions with nearly similar accuracy which agreed with the study made by Baliyan *et al.* [5].

#### Regarding the type of lesions

Benign fluid focal lesions (hemangiomas and cysts) in this study show hyperintensity on the DWI image and also hyperintensity on the ADC map, the pattern known as 'T2 shine-through.' This was stated also by Tokgoz *et al.* [9]. Benign solid focal lesions are not or only slightly distinguishable from the liver

Figure 1



Axial T1WI (a), T2WI (b), postcontrast T1WI (c) cirrhotic liver; segment II subcapsular area hypointense in T1, inconspicuous in T2 with intense enhancement. DWIs:  $b=500$  (d),  $b=1000$  (e); appeared bright and became brighter with increasing  $b$  values. ADC:  $1.05 \times 10^{-3} \text{mm}^2/\text{s}$ . Diagnosis: hepatocellular carcinoma. ADC, apparent diffusion coefficient.



parenchyma on the DWI at higher *b* values and are isointense or slightly hyperintense compared with the surrounding liver on the ADC map [9].

Malignant focal lesions, such as HCC nodules or metastases, present a pattern known as 'restricted diffusion' that is hyperintensity on the DWI image and hypointensity on the ADC map [10].

It was noted in our study that benign hepatic lesions have generally higher ADC values compared with malignant lesions, which agreed with what Calistri *et al.* [8] stated.

Variable degrees of overlap were noted with no definite cutoff value and this was mentioned in other studies [10].

Different ADC cutoffs ( $1.59 \times 10^{-3} \text{mm}^2/\text{s}$ ) by Kaya and Koc [2] and ( $1.4\text{--}1.6 \times 10^{-3} \text{mm}^2/\text{s}$ ) in Chen *et al.* [3] have been described in the literature.

Although there is no definite ADC cutoff value, our study showed findings similar to those found in other studies as:

- (1) Cysts had the highest mean ADC values in the present study ( $2.4 \pm 0.80 \times 10^{-3} \text{mm}^2/\text{s}$ ), which was in line with other studies as Wei *et al.* [4] with a mean ADC value of  $3.40 \pm 0.48 \times 10^{-3} \text{mm}^2/\text{s}$ ; Jahic *et al.* [6] with a mean ADC value of 2.5

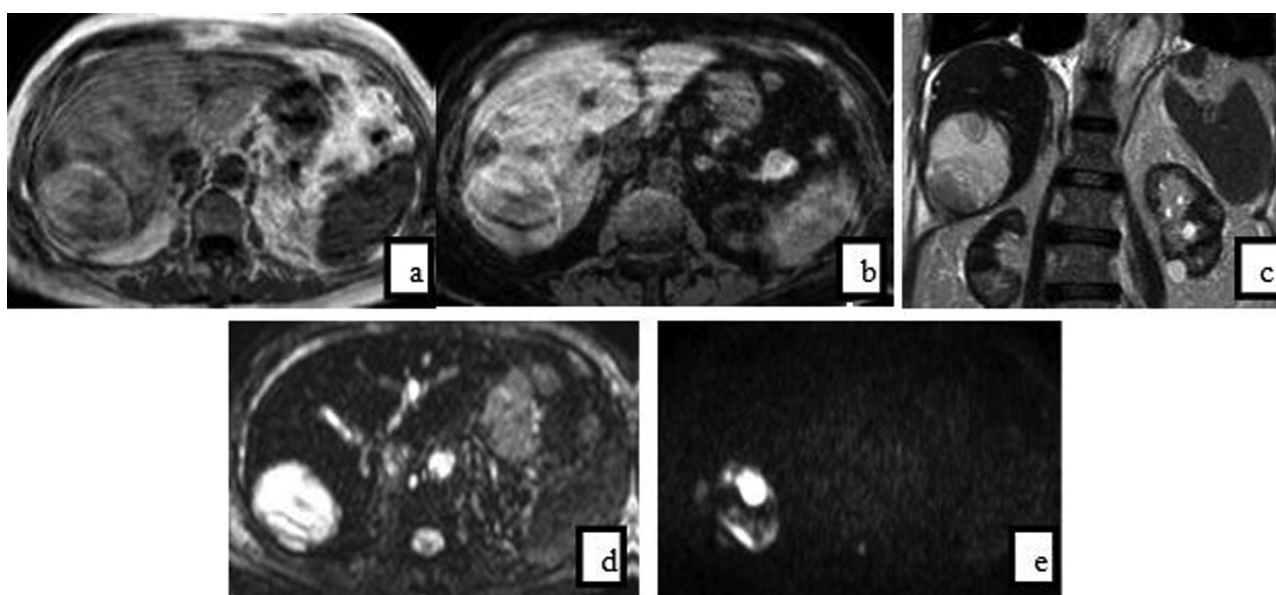
$\pm 0.31 \times 10^{-3} \text{mm}^2/\text{s}$ ; and Calistri *et al.* [8] with a mean ADC value of  $2.61 \pm 0.45 \times 10^{-3} \text{mm}^2/\text{s}$  (Fig. 2).

- (2) The lowest ADC values belonged to metastases with a mean ADC value of  $1.055 \pm 0.155 \times 10^{-3} \text{mm}^2/\text{s}$ . This data is similar to Jahic *et al.* [6] with a mean ADC value of  $1.00 \pm 0.22 \times 10^{-3} \text{mm}^2/\text{s}$ ; Calistri *et al.* [8] with a mean ADC value of  $1.50 \pm 0.65 \times 10^{-3} \text{mm}^2/\text{s}$ ; and Colagrande *et al.* [7] with a mean ADC value of  $1.2 \pm 0.5 \times 10^{-3} \text{mm}^2/\text{s}$ .

There was significant overlap between ADC values of adenoma (mean ADC value of  $1.28 \pm 0.13 \times 10^{-3} \text{mm}^2/\text{s}$ ) and ADC values of different malignant lesions. Unfortunately, it was not possible to differentiate between them on the basis of their ADC values nor on their appearance on DWIs, as they all show restricted diffusion (Fig. 3). This data was in line with Bioulac-Sage *et al.* [11], who found considerable overlap of solid benign and solid malignant lesions and stated that there were no statistically significant differences in ADC values between hepatic adenomas, FNH, cholangiocarcinoma, and HCC. However, Angello *et al.* [12] stated that the ADC values were significantly greater with focal nodular hyperplasia than with adenomas and with a cutoff value of  $1.37 \times 10^{-3} \text{mm}^2/\text{s}$ .

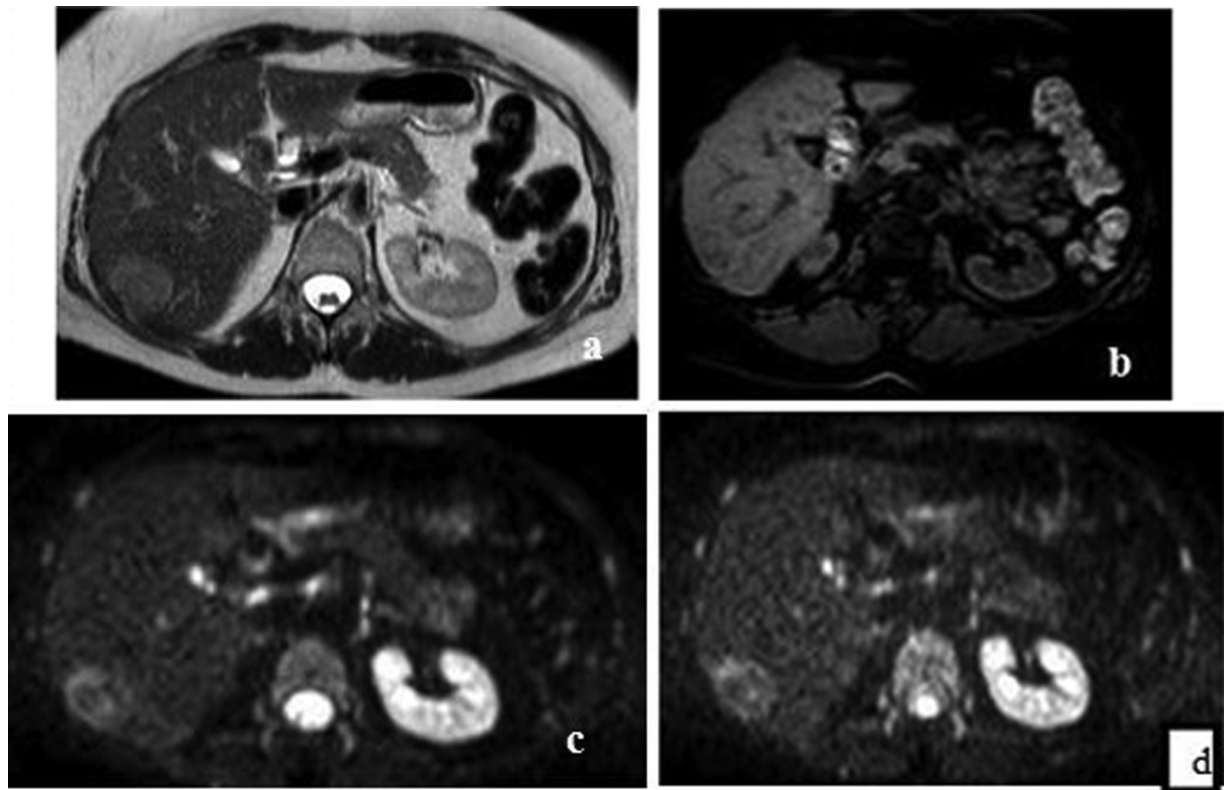
The ADC value detected for HCC which was the most common primary malignant liver lesion ranged from

Figure 2



Case of right hepatic lobe focal lesion in ultrasound. T1WI (a), T1WI-fat-sat (b), T2WI (c), segment VI focal lesion; heterogenous hemorrhagic lesion. DWIs: b500 (d), b1000 (e); heterogeneous bright with less brightness in high *b* values. ADC:  $1.6 \times 10^{-3} \text{mm}^2/\text{s}$ . Diagnosis: hemorrhagic cyst. ADC, apparent diffusion coefficient.

Figure 3



Female; history of oral contraceptive pills. T2WI(a), T1WI fat-sat (b); segment VI focal lesion; hyperintense T2 and hypointense T1-fat-sat denoting fatty content. DWIs: b500 (c) and b1000 (d); bright with different b values. ADC:  $1.41 \times 10^{-3} \text{mm}^2/\text{s}$ . Diagnosis: adenoma (pathologically proven). ADC, apparent diffusion coefficient.

$1.05 \times 10^{-3}$  to  $1.38 \times 10^{-3} \text{mm}^2/\text{s}$ , which was nearly similar to  $1.1 \pm 0.31 \times 10^{-3} \text{mm}^2/\text{s}$  stated by Shankar *et al.* [13].

Since there can be substantial overlap in the range of ADCs between different pathologies, the ADC should be interpreted concurrently with all available imaging before making the radiologic diagnosis and this was mentioned in other studies such as that of Parsai *et al.* [14].

### Conclusion

Diffusion-weighted MRI sequence with quantitative ADC measurements should be used as an additional sequence to supplement conventional MRI protocol studies for proper characterization of focal hepatic lesions putting into consideration an overlap range.

### Acknowledgements

The study was primarily carried out at Kasr El-Aini Hospital.

### Financial support and sponsorship

Nil.

### Conflicts of interest

There are no conflicts of interest.

### References

- 1 Caraiani C, Chiorean L, Fenesan D, Lebovici A, Feier D, Gersak M, *et al.* Diffusion weighted magnetic resonance imaging for the classification of focal liver lesions as benign or malignant. *J Gastrointest Liver Dis* 2015; 24:309–317.
- 2 Kaya B, Koc Z. Diffusion-weighted MRI and optimal b-value for characterization of liver lesions. *Acta Radiol* 2014; 55: 532–542.
- 3 Chen ZG, Xu L, Zhang SW, Huang Y, Pan RH. Lesion discrimination with breath-hold hepatic diffusion-weighted imaging: a meta-analysis. *World J Gastroenterol* 2015; 21:1621–1627.
- 4 Wei C, Tan J, Xu L, Juan L, Zhan SW, Wang L, *et al.* Differential diagnosis between hepatic metastases and benign focal lesions using DWI with parallel acquisition technique: a meta-analysis. *Tumour Biol* 2015; 36:983–990.
- 5 Baliyan V, Das CJ, Sharma R, Gupta AK. Diffusion weighted imaging: technique and applications. *World J Radiol* 2016; 8:785–798.
- 6 Jahic E, Sofic A, Selimovic AH. DWI/ADC in differentiation of benign from malignant focal liver lesion. *Acta Inform Med* 2016; 24:244–247.
- 7 Colagrande S, Castellani A, Nardi C, Lorini C, Calistri L, Filippone A. The role of diffusion-weighted imaging in the detection of hepatic metastases from colorectal cancer: a comparison with unenhanced and Gd-EOB-DTPA enhanced MRI. *Eur J Radiol* 2016; 85:1027–1034.
- 8 Calistri L, Castellani A, Matteuzzi B, Mazzoni E, Pradella S, Colagrande S. Focal liver lesions classification and characterization: what value do DWI and ADC have? *J Comput Assist Tomogr* 2016; 40:701–708.
- 9 Tokgoz O, Unlu E, Unal I, Serifoglu I, Oz I, Aktas E, *et al.* Diagnostic value of diffusion weighted MRI and ADC in differential diagnosis of cavernous hemangioma of the liver. *Afr Health Sci* 2016; 16:227–233.
- 10 Caraiani CN, Marian D, Militaru C, Calin A, Badea R. The role of the diffusion sequence in magnetic resonance imaging for the differential diagnosis between hepatocellular carcinoma and benign liver lesions. *Clujul Med* 2016; 89:241–249.

- 11 Bioulac-Sage P, Sempoux C, Balabaud C. Hepatocellular adenoma: classification, variants and clinical relevance. *Semin Diagn Pathol* 2017; 34:112–125.
- 12 Agnello F, Ronot M, Valla DC, Sinkus R, Van Beers BE, Vilgrain V. High-b-value diffusion-weighted MR imaging of benign hepatocellular lesions: quantitative and qualitative analysis. *Radiology* 2012; 262:511–519.
- 13 Okamura S, Sumie S, Tonan T, Nakano M, Satani M, Shimose S, *et al.* Diffusion-weighted magnetic resonance imaging predicts malignant potential in small hepatocellular carcinoma. *Dig Liver Dis* 2016; 48:945–952.
- 14 Parsai A, Zerizer I, Roche O, Gkoutzios P, Miquel ME. Assessment of diffusion-weighted imaging for characterizing focal liver lesions. *Clin Imaging* 2015; 39:278–284.